

Non-Landau level cyclotron orbits and the quantum Hall effect in Harper-Hofstadter bands

David Bauer,^{*} Fenner Harper, and Rahul Roy

*Department of Physics and Astronomy, University of California at Los Angeles,
475 Portola Plaza, Los Angeles, California 90095, USA*

(Dated: August 21, 2018)

Recent developments in fractional quantum Hall (FQH) physics suggest the importance of studying FQH phases of particles occupying single-particle states that are not Landau levels. FQH phases in the regime of strong lattice effects, called fractional Chern insulators (FCI), provide one setting for such studies. As the strength of lattice effects vanishes, the bands of generic lattice models asymptotically approach Landau levels. In this article, we construct non-generic lattice models for single-particle bands that are distinct from Landau levels even in this asymptotic limit. In particular, we study a finely-tuned model with effective continuum hamiltonian with purely quartic dependence on momentum. We describe how the distinction between such bands and Landau levels may be quantified by magnetic Brillouin zone (MBZ) geometry, and we compare the stability of FQH phases in various regimes.

I. INTRODUCTION

The incompressible liquid phases of the fractional quantum Hall effect (FQHE) serve as prototypical examples of topologically ordered or gapped quantum liquid phases^{1,2} in 2+1 dimensions. These phases are characterized by their long-range entanglement structure, which gives rise to topological quasiparticles and universal, quantized linear responses. Theoretical models of the quantum Hall (QH) fluid – based, for example, on model wavefunctions³ – often make the simplifying assumption that the microscopic constituent particles occupy states in a single Landau level. Some properties of Landau levels, such as nonzero Chern number,⁴ are essential for the QHE, but recent work points to a need to understand the QHE in the case that the single-particle states are not Landau levels.

Among such work is the observation, due to Haldane, that the FQH fluid carries an emergent geometrical degree of freedom⁵ corresponding to the shape of elementary composite particles or ‘droplets.’⁶ The geometry of the FQH fluid manifests in part through universal contributions to linear responses corresponding to perturbative variations in geometry, of which the Hall viscosity^{7–10} is an example. In topological fluids, the Hall viscosity has a universal part proportional to the topological spin of the fluid,⁹ which is related to the composite droplet shape.⁶ This geometrical degree of freedom may be obscured by the introduction of non-generic symmetries to the FQH problem implicitly, via the assumption that the underlying single-particle bands are Landau levels.

The study of the FQH beyond Landau levels has also been spurred by the discovery of fractional Chern insulators (FCI) – time-reversal (TR) symmetry-breaking, fractionalized phases observed in the regime of strong lattice effects.^{11,12} In this regime, the single-particle states reside in Chern bands rather than Landau levels. The addition of a non-negligible lattice potential introduces additional geometric data that may break some non-generic symmetries. For example, in the case of a square lattice, $SO(2)$ rotational invariance in the coordinate plane is explicitly broken to C_4 lattice symmetry. From this point of view, a complete theory of the FQHE formulated as generically as possible should furnish a theory of FCI phases. Understanding how the lattice potential of FCIs affects the geometrical responses of their topological fluid states is an active

research subject.¹³

In this article, we study the geometry of Chern bands over the magnetic Brillouin zone (MBZ) parameterizing eigenstates of magnetic translations operators.¹⁴ While this geometry is distinct from the emergent, many-body geometry of the FQH fluid, studies of FCIs have described how single-particle geometry influences the stability of many-body FQH phases through the GMP/ w_∞ algebra of band-projected density operators.^{12,15–17} This connection is substantiated by numerical studies,^{18–20} and researchers have employed it to engineer ‘ideally’ stable FCI models.²¹ Chern band geometry can also be understood as the lattice analogue of the continuum, cyclotron-orbit geometry studied in Ref. 22.

Experimental signatures of FCIs have been observed in a system of interacting electrons coupled to a superlattice potential generated in a bilayer graphene heterostructure.²³ The electrons in the superlattice form Harper-Hofstadter bands with non-zero Chern number. At fractional fillings corresponding to Laughlin states in the conventional FQHE, a gapped phase with fractionally-quantized Hall conductance is observed.²³ Other experimental works have identified single-particle Chern bands in the FCI regime.^{24–26} Chern bands can be realized in periodically-driven quantum or Floquet systems and their Berry curvature engineered and measured.²⁷

but FCIs redoubled interest in the subject with the promise of realizing FQH phases outside the usual 2DEG regime. The distinction between FCI models and Harper-Hofstadter^{30–32} models for lattice electron gasses is nominally that the former have no *net* magnetic field per unit cell, as in the Haldane Chern insulator model.³³ From a theoretical point of view, this distinction is unnecessary,³⁴ and we view FCIs simply as the limit of Harper-Hofstadter models when lattice effects are strong.

In this article, we discuss Hofstadter-like tight-binding models with additional, longer-range hoppings, in particular focusing on the relationship between the continuum limit of these models and the Landau level hamiltonian. As we will argue in the following section, the bands of such models will generically reproduce Landau levels in the continuum limit. Our main result is to construct such a model that does not have Landau levels as its effective continuum bands. In particular,

by adding an additional next-nearest-neighbor hopping term with a negative hopping amplitude, we tune the effective continuum hamiltonian so that the quadratic term vanishes, giving a hamiltonian quartic in momentum to lowest order. This provides a novel setting in which to study quantum Hall systems that is distinct from both the FCI and continuum 2DEG regimes. We focus mainly on a particular choice of hopping amplitudes for the sake of concreteness, but note that different choices of hopping amplitudes lead to an infinite family of non-Landau level continuum bands. We discuss the Chern band geometry of this non-Landau level model, which we use to quantify differences between these bands and Landau levels. We study the stability of the $\nu = 1/3$ Laughlin phase by numerical exact diagonalization of a repulsive, many-body hamiltonian projected to the lowest band of this lattice model, and we observe the signatures of the Laughlin phase in the spectrum of the many-body hamiltonian. We focus mainly on the weak-field, effective continuum limit behavior, although some of our numerics should be relevant to fractional Chern insulators.

II. PRELIMINARY DISCUSSION

A. Landau levels

Since Landau levels serve as our prototype for more general Chern bands, we begin by briefly recalling some physics of Landau levels.¹ We study a single electron in two dimensions in the presence of a uniform, perpendicular magnetic field B . The single-particle hamiltonian for non-zero B is

$$H_0 = \frac{1}{2m} (\pi_x^2 + \pi_y^2), \quad (1)$$

where $\pi_a = p_a - eA_a(\mathbf{r})$ is the gauge-covariant dynamical momentum and p_a is the gauge-invariant canonical momentum. The operators H_0 , π_1 and π_2 form a three-dimensional Heisenberg Lie algebra \mathfrak{h} , with commutators $[H_0, \pi_1] = [H_0, \pi_2] = 0$, and $[\pi_1, \pi_2] = i\hbar^2\ell^{-2}$, where we have introduced the *magnetic length* $\ell = \sqrt{\frac{\hbar}{eB}}$.

We then define *guiding-center position operators*

$$R_a = r_a - \frac{\ell^2}{\hbar} \epsilon_{ab} \pi_b,$$

which obey commutation relations $[R_a, R_b] = i\ell^2 \epsilon_{ab}$ and $[R_a, \pi_b] = 0$, and $[H_0, R_a] = 0$, so that the guiding-center and cyclotron operators each form distinct Heisenberg algebras. This decomposition holds in any gauge, although the specific expressions for R_a , R_b , and H_0 in terms of the gauge-invariant positions and momenta r_a , p_a depend on the gauge choice.

We obtain representations of the Heisenberg algebras by a choice of Fock or ladder operators, which are complex linear combinations of the position operators satisfying

$$\begin{aligned} [a(\boldsymbol{\pi}), a^\dagger(\boldsymbol{\pi})] &= 1, \\ [b(\mathbf{R}), b^\dagger(\mathbf{R})] &= 1. \end{aligned}$$

This choice is equivalent to a choice of linear complex structure on the respective coordinate spaces. The states

$$|n, m\rangle = \frac{(a^\dagger)^n}{\sqrt{n!}} \frac{(b^\dagger)^m}{\sqrt{m!}} |0, 0\rangle. \quad (2)$$

form a basis for the Hilbert space. For the Landau level hamiltonian (1), we may choose the cyclotron Fock operators a , a^\dagger such that

$$H_0 = \hbar\omega (a^\dagger a + aa^\dagger).$$

Since the hamiltonian is central with respect to both Heisenberg algebras, the basis states $|n, m\rangle$ are eigenstates of H_0 :

$$H_0 |n, m\rangle = \hbar\omega \left(a^\dagger a + \frac{1}{2} \right) |n, m\rangle.$$

A generic state $|n, \Psi\rangle$ within the n th Landau level can be written as a function purely of the b^\dagger operators applied to the vacuum state:

$$|n, \Psi\rangle = \Psi(b^\dagger) |n, 0\rangle.$$

B. Effective Landau levels from weak-field Harper-Hofstadter models

In this section, we consider the weak-field limit $\phi \rightarrow 0$ of a Harper-Hofstadter tight-binding hamiltonian, and show that to lowest order in ϕ , this hamiltonian reproduces the Landau level hamiltonian

We introduce a uniform background magnetic field B perpendicular to the spatial extent of the lattice. We choose the value of B to be such that the flux per lattice plaquette is $\phi = Ba^2 = \frac{P}{Q}\phi_0$, where $\phi_0 = 2\pi\hbar/e$ is the magnetic flux quantum and P and Q are relatively prime integers. We will mostly have in mind the case $P = 1$, in which the band structure is on conceptually simplest.³⁵ In terms of the magnetic length and lattice spacing, $\phi = \hbar a^2/(e\ell^2)$. For the rest of this article, we will work in units in which $\hbar/e = 1$, so that $\phi = a^2/\ell^2$ is a dimensionless ratio of length scales.

In the presence of the magnetic field, the naive translation operators are not gauge invariant,² and we must accompany translations by compensatory gauge transformations. The gauge invariant translation operators are

$$T_a = \sum_{\mathbf{m}} e^{i\theta_a(\mathbf{m})} c_{\mathbf{m}+\mathbf{e}_a}^\dagger c_{\mathbf{m}}.$$

where the phases $e^{i\theta_a(\mathbf{m})}$ satisfy

$$\theta_1(\mathbf{m}) + \theta_2(\mathbf{m} + \mathbf{e}_1) - \theta_1(\mathbf{m} + \mathbf{e}_2) - \theta_2(\mathbf{m}) = \phi,$$

We regard the phases θ as residing on the links of the lattice, but we canonically identify $\theta_a(\mathbf{m}) = \theta(\mathbf{m}, \mathbf{m} + \mathbf{e}_a)$. The components of \mathbf{T} do not commute, but satisfy

$$T_x T_y = \exp(i\phi) T_y T_x.$$

The lattice translation operators T_a are unitary, so we can write them in terms of hermitian generators $T_a = \exp[iK_a]$. The K_a are the lattice analogues of the covariant momentum operators π_a , and we will sometimes call them mometa for brevity. These operators have the commutator

$$[K_x, K_y] = \phi.$$

The most general tight-binding hamiltonian we can write down has non-zero hopping amplitudes between any two sites of the lattice. However, the non-commutativity of the T_a leads to an ambiguity in constructing this hamiltonian when $B \neq 0$. We resolve this ambiguity by specifying that the operator for hopping j sites in the x direction and j sites in the y direction be the symmetric sum $T_x^j T_y^k + T_y^k T_x^j$, so that our hamiltonian is

$$H_{\text{TB}} = - \sum_{j,k} t_{jk} (T_x^j T_y^k + T_y^k T_x^j) + \text{h.c.}$$

We could also have resolved this ambiguity by a gauge choice, although for now we maintain gauge symmetry. We note that in our notation, the hopping amplitudes t_{jk} are always real, and any complex phase factors come from the action of the translation operators.

Let us look at just the nearest-neighbor (NN) hopping hamiltonian containing only first powers of the translation operators,

$$H_{\text{NN}} = -t_{10} (T_x + T_x^\dagger) - t_{01} (T_y + T_y^\dagger)$$

In the C_4 symmetric case, $t_{01} = t_{10}$, H_{NN} is just the hamiltonian of the usual Hofstadter model with non-zero amplitude only for NN hoppings. Since $T_a = e^{iK_a}$,

$$H_{\text{NN}} = -2t_{10} \cos(K_x) - 2t_{01} \cos(K_y).$$

In order to make the dependence on ϕ explicit, we rescale the K_a operators, defining $\sqrt{\phi} P_a = K_a$.

$$\begin{aligned} H_{\text{NN}} &= -2 \sum_{n=0}^{\infty} \frac{(-1)^n \phi^n}{(2n)!} (t_{10} P_x^{2n} + t_{01} P_y^{2n}) \\ &= -2 + 2\phi \frac{(t_{10} P_x^2 + t_{01} P_y^2)}{2} + O(\phi^2). \end{aligned}$$

Now let $t' = \alpha^2 t$, i.e., t is a common hopping energy scale and α parameterizes anisotropy in the hopping amplitudes. Then to lowest order in ϕ , we have a small- ϕ effective hamiltonian $H_{\text{eff}} = t\phi (P_x^2 + \alpha^2 P_y^2)$. We can rewrite this in terms of momentum operators that satisfy $[\pi_x, \pi_y] = i\hbar e B$ as

$$H_{\text{eff}} = \frac{1}{2m_*} (\pi_x^2 + \pi_y^2),$$

showing that our effective hamiltonian is isomorphic to the Landau level hamiltonian with effective mass $m_* = \hbar^2/(2ta^2\alpha)$. In order to recover all of the physics of Landau levels, we also need an analogue of the guiding-center operators that commute with the hamiltonian but not one another, producing an extensive degeneracy. Here, this role is filled

by the magnetic translation operators, which we define in the following section. If we consider not just nearest-neighbor but also longer range hopping terms, the details of the above argument are slightly more complicated, but to lowest order the hamiltonian is quadratic in the momenta. This gives us an effective mean-field hamiltonian for the cyclotron degrees of freedom.

C. Chern band geometry

Instead of the continuous translation symmetry that generates degenerate states in Landau levels in infinite plane and toroidal geometries, our system has discrete translation symmetry corresponding to the magnetic translation operators U_a . If we define a magnetic unit cell (MUC) with dimensions $X_{\text{MUC}} \times Y_{\text{MUC}} = A_{\text{MUC}}$ enclosing flux $\phi = 1$, translations by one MUC in either direction commute with each other and the hamiltonian. The simultaneous eigenstates of the hamiltonian and MUC translations are $|n, \mathbf{k}\rangle$, where \mathbf{k} takes values in the magnetic Brillouin zone and n labels eigenstates of H . We can write the hamiltonian

$$H = \sum_n \int d^2k E_n(\mathbf{k}) P_{n,\mathbf{k}}, \quad (3)$$

where E_n is the dispersion of the n -th band of the hamiltonian, and $P_{n,\mathbf{k}}$ is the projector onto the state $|n, \mathbf{k}\rangle$.

Unlike in Landau levels, the dispersion $E_n(\mathbf{k})$ generically has some finite width, and the states in the band are not exactly degenerate. In the weak-field case this bandwidth will be exponentially small,³⁵ while in the strong-field limit we may follow the usual procedure of adding long-range hoppings to flatten the band.^{11,12} In either case, we will neglect the bandwidth. Despite being dispersionless, these Chern bands are distinct from Landau levels. We can quantify this distinction by considering the Berry curvature and Fubini-Study (FS) metric defined on the magnetic Brillouin zone.^{12,17,19} (The FS metric has also been called the Bures metric in this context.³⁶) For notational simplicity, we define $\partial_a = \partial_{k_a}$. Then, respectively, the Berry curvature and FS metric components for a band with projector $P_{\mathbf{k}}$ are

$$B(\mathbf{k}) = \epsilon_{ab} \text{Tr}(\partial_a P_{\mathbf{k}} \partial_b P_{\mathbf{k}}),$$

and, defining the orthogonal projector $Q_{\mathbf{k}} = 1 - P_{\mathbf{k}}$,

$$g_{ab}(\mathbf{k}) = \frac{1}{2} \text{Tr}(\partial_a Q_{\mathbf{k}} \partial_b P_{\mathbf{k}} + \partial_b Q_{\mathbf{k}} \partial_a P_{\mathbf{k}}).$$

The traces in these expressions are taken over the cyclotron Hilbert space. The TR-symmetry breaking Chern bands that we want to study are those with nonvanishing first Chern number

$$c_1 = \int d^2k B(\mathbf{k}).$$

The FS metric and Berry curvature for any band obey the inequalities¹⁷

$$\begin{aligned} \text{Det } g(\mathbf{k}) &\geq \frac{1}{4}|B(\mathbf{k})|^2 \\ \text{Tr } g(\mathbf{k}) &\geq |B(\mathbf{k})|, \end{aligned}$$

which we call the *determinant inequality* and *trace inequality* respectively. For Landau levels, these inequalities are saturated. The degree to which the FS metric and Berry curvature for a particular band saturate these inequalities therefore provides a quantitative measure of deviations from Landau level behavior and may also provide a measure of stability of FQH phases in the band. We define

$$\begin{aligned} D(\mathbf{k}) &= \text{Det } g(\mathbf{k}) - \frac{1}{4}|B(\mathbf{k})|^2 \\ T(\mathbf{k}) &= \text{Tr } g(\mathbf{k}) - |B(\mathbf{k})|, \end{aligned}$$

measuring the degree of saturation, and we will sometimes refer to these quantities as the determinant and trace inequalities, respectively.

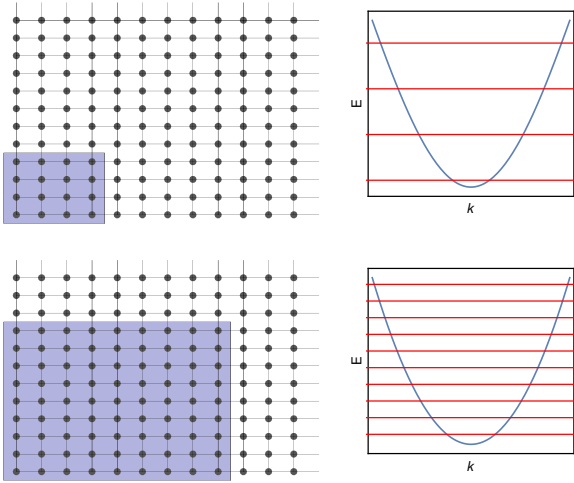


FIG. 1. Schematic depiction of Landau-levels as the weak-field limit of Harper-Hofstadter bands near the minimum of a periodic potential. As the flux per plaquette is decreased, the elementary magnetic unit cell – represented by the blue region of the lattice – must increase in size to enclose the same number of flux quanta. In turn, the number of states in within each band decreases, and each band comprises states increasingly close to the minimum of the zero-field dispersion.

The weak-field/continuum limit is implemented in the \mathbf{k} -representation by expanding the band dispersion $E_n(\mathbf{k})$ near a band minimum. The lowest-order term in such an expansion will generically be quadratic in \mathbf{k} , which essentially follows from our argument in the previous section. Since the mean electron density ρ_0 in QH systems is pegged to the magnetic flux density by the filling fraction

$$\nu = \frac{N_p}{N_s} = N_p \frac{A_{\text{tot}}}{A_{\text{MUC}}}$$

the weak-field limit corresponds to the limit of a dilute electron fluid. This leads to a more conceptual picture, shown in cartoon form in Fig. 1 for how decreasing flux per plaquette leads to continuum limit Landau levels. If we fix the overall system size and the magnetic flux attached to each guiding-center lattice site (the flux through each MUC), decreasing flux per plaquette must increase the area of each MUC. We therefore increase the number of states in the cyclotron Hilbert space, while decreasing the number of guiding-center states available within each band. The states that live near the band minimum when there is no magnetic field then redistribute into increasingly higher bands as ϕ decreases.

III. NON-LANDAU EFFECTIVE HAMILTONIANS

In this section, we introduce and study a new class of weak-field effective hamiltonians that cannot be transformed into the Landau hamiltonian at lowest order in ϕ . To start, we consider the following tight-binding hamiltonian obtained by adding a next-nearest-neighbor (NNN) hopping to the Hofstadter model:

$$\begin{aligned} H_{\text{TB}} &= -t_1 (T_x + T_x^\dagger + T_y + T_y^\dagger) \\ &\quad - t_2 (T_x^2 + T_x^{\dagger 2} + T_y^2 + T_y^{\dagger 2}). \end{aligned} \quad (4)$$

For this particular model, we have omitted the NNN hopping diagonally across the elementary plaquette. Unless explicitly stated, we will assume from here onward that t_1 sets the overall scale of the hamiltonian, and set $t_1 = 1$; the remaining hopping amplitudes in each expression should then be understood as dimensionless ratios.

As in Section II B, we write this in terms of the hermitian generators of lattice translations,

$$\begin{aligned} H_{\text{TB}} &= -2 (\cos(K_x) + \cos(K_y)) \\ &\quad - 2t_2 (\cos(2K_x) + \cos(2K_y)) \end{aligned}$$

Replacing the cosine terms by their Taylor expansion, the terms lowest-order in the momenta are

$$\begin{aligned} H_{\text{TB}} &= -4 - 4t_2 + (1 + 4t_2) (K_x^2 + K_y^2) \\ &\quad - \left(\frac{1}{12} + \frac{4}{3}t_2 \right) (K_x^4 + K_y^4) + \dots \end{aligned}$$

If we make the particular choice of hopping amplitudes $t_2 = -1/4$, then the quadratic terms vanish exactly, and we are left with an effective hamiltonian that is quartic in the momenta to lowest order,

$$H_{\text{eff}} = -3 + \frac{1}{4} (K_x^4 + K_y^4). \quad (5)$$

We will refer to this tight-binding model and its effective continuum limit as the ‘zero-quadratic’ model. The negative hopping amplitude necessary to eliminate the quadratic term can in be realized in optical lattice experiments by periodic shaking of the lattice.³⁷ Unlike the Landau level hamiltonian, this hamiltonian does not have $SO(2)$ rotational symmetry, but it

is symmetric under the square lattice point group D_4 . We note that the particular quartic momentum operator in (5) can be written

$$K_x^4 + K_y^4 = (K_x^2 + K_y^2)^2 - (K_x^2 K_y^2 + K_y^2 K_x^2),$$

that is, as the square of the Landau-level hamiltonian plus a term that explicitly breaks the rotational symmetry.

We now consider some details of the model given by Eq. (4), in particular its continuum limit. We plot the energy eigenvalues obtained from the Harper-type equation for this model as a function of ϕ – the analogue of the Hofstadter “butterfly” for this model³² and display this in Fig. 2. In the Hofstadter model, where the bands appear approximately linear in ϕ near $\phi = 0$, the present model has bands that are roughly quadratic in ϕ in this region. We compute the Berry curvature and Chern number of these bands for $\phi = \frac{1}{N}$ and verify that they have Chern number $|c_1| = 1$.

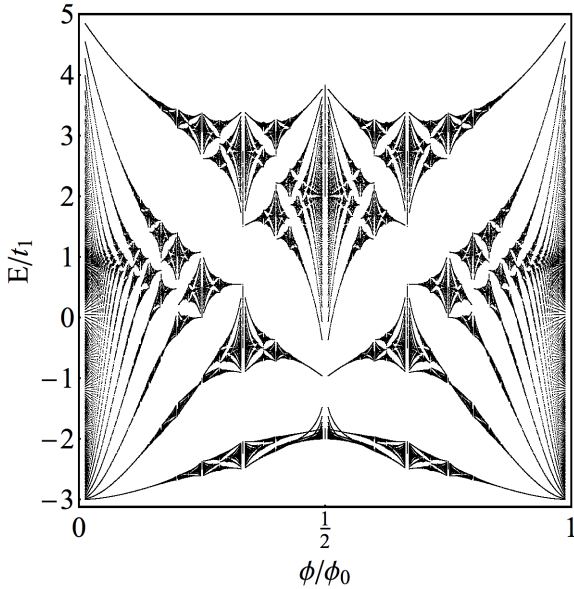


FIG. 2. Energy eigenvalues of the lattice Harper-Hofstadter hamiltonian (4) with $t_1 = 1$, $t_2 = -1/4$ as a function of magnetic flux per elementary lattice plaquette $\phi = P/Q$.

As in the Landau level problem, we study the spectrum of this model by introducing ladder operators a , a^\dagger corresponding to the cyclotron momenta K_a . For example, we choose the operators

$$a = \frac{1}{\sqrt{2\phi}} (K_x - iK_y),$$

$$a^\dagger = \frac{1}{\sqrt{2\phi}} (K_x + iK_y),$$

with inverse map

$$K_x = \sqrt{\frac{\phi}{2}} (a + a^\dagger),$$

$$K_y = -i\sqrt{\frac{\phi}{2}} (a - a^\dagger).$$

We also define the dimensionless operator

$$h_0 = \left(a^\dagger a + \frac{1}{2} \right).$$

In terms of these operators,

$$(K_x^2 + K_y^2)^2 = 4\phi^2 h_0^2,$$

$$(K_x^2 K_y^2 + K_y^2 K_x^2) = \phi^2 \left(h_0^2 - \frac{1}{2} (a^4 + a^{\dagger 4}) - \frac{3}{4} \right),$$

and the effective hamiltonian is

$$H_{\text{eff}} = \frac{\phi^2}{8} \left[(a^4 + a^{\dagger 4}) + 6h_0^2 + \frac{3}{2} \right]. \quad (6)$$

We numerically approximate this hamiltonian by working in a basis of number eigenstates $|n\rangle$ satisfying $a^\dagger a |n\rangle = n |n\rangle$ and truncating to a finite-dimensional subspace. This gives estimates for the cyclotron energies and overlaps with the Landau level states. We find good agreement between this continuum approximation truncated to $n \leq 1000$ and exact numerical energy levels of lattice hamiltonian for small ϵ . The first two nonzero overlaps of the ground state $|\tilde{0}\rangle$ of the hamiltonian (6) with the Landau level states are $\langle \tilde{0} | 0 \rangle \approx 0.9991$, $\langle \tilde{0} | 4 \rangle \approx -0.0422$. When expressed with ladder operators, the trace inequality takes the particularly simple form $\langle T \rangle = 2 \langle a^\dagger a \rangle$,²⁰ that is, $\langle T \rangle$ is twice the mean LL occupation number n_0 . Calculating this in the truncated Landau level basis, we find $\langle T \rangle \approx 0.0143$, in good agreement with the value found from integrating the lattice $T(\mathbf{k})$ over the MBZ, $\langle T \rangle \approx 0.0145$.

We also study the spectrum of cyclotron orbits of this hamiltonian semiclassically by applying the Bohr-Sommerfeld quantization condition that the adiabatic invariants of the classical hamiltonian be quantized. In our notation, this condition takes the form

$$\oint_{H=E_n} K_x dK_y = 2\pi n,$$

with the integral taken over a closed curve of constant energy in classical phase space. From this condition we find

$$E_n \sim n^2 \phi^2,$$

in agreement both with the numerically-obtained, approximate spacing of the cyclotron levels, and with the quadratic dependence of E on ϕ observed in the butterfly plot, Fig. 2.

We now consider general values of t_2 . In this case, the effective hamiltonian is

$$H_{\text{eff}} = -\frac{1+16t_2}{12} (K_x^4 + K_y^4) + (1+4t_2) (K_x^2 + K_y^2), \quad (7)$$

or

$$H_{\text{eff}} = 2\phi(1+4t_2) h_0 - \phi^2 \frac{(1+16t_2)}{4} \left(h_0^2 + \frac{(a^4 + a^{\dagger 4})}{6} + \frac{1}{4} \right).$$

For any value of t_2 away from the fine-tuned point $t_2 = -1/4$, we may always choose ϕ small enough that the quadratic term dominates and we recover the Landau level hamiltonian. However, if we consider ϕ small but fixed, we can make the weight of the quadratic term small by tuning t_2 appropriately. In this regime, we can treat the quadratic term in the hamiltonian as a perturbation to the quartic term, with perturbative parameter

$$\varepsilon = \frac{8}{\phi} \frac{(1 + 4t_2)}{(1 + 16t_2)}.$$

A weak upper bound on the regime in which may treat the quadratic term as a perturbation is given by setting $\varepsilon < 1$ or

$$t_2 > -\frac{1}{4} + \frac{3}{32}\phi + O(\phi^2).$$

In Fig. 3, we plot $\langle T \rangle$ for the lowest band of this hamiltonian for various values of t_2 , including values that interpolate between the Hofstadter model and our zero-quadratic model. For large values of ϕ , this plot shows a clear local minimum, which we interpret to be the point where the weight of h_0 and its powers are maximized. As ϕ decreases, $\langle T \rangle$ flattens toward zero for t_2 near the Hofstadter regime, in line with asymptotic vanishing of $\langle T \rangle$ in the Hofstadter model.²⁰

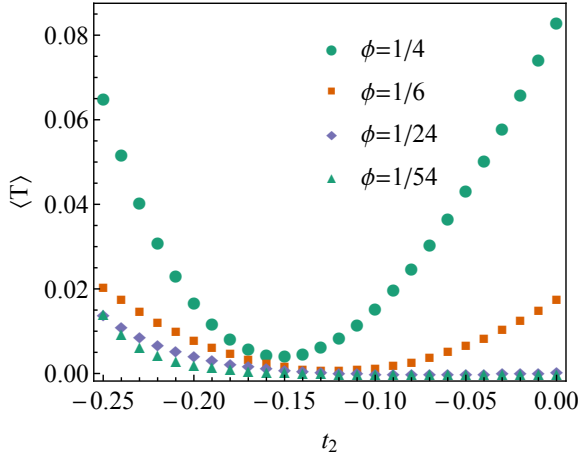


FIG. 3. Magnetic Brillouin zone-averaged trace inequality $\langle T \rangle$ for the lowest-lying band of (4) as a function of t_2 with $t_1 = 1$. For $t_2 = 0$ this is the Hofstadter model, while $t_2 = -1/4$ gives the fine-tuned zero-quadratic model with effective hamiltonian (5).

By introducing additional hopping amplitudes between non-neighboring sites and tuning the amplitudes appropriately, we may eliminate increasingly higher-order terms in the hamiltonian. We focus on the case in which we add only straight-line hoppings, as we did for the zero-quadratic model above. For example, we obtain the effective hamiltonian

$$H_{\text{eff}} = -\frac{4}{3} + \frac{K_x^6 + K_y^6}{15}$$

by choosing $t_{20} = t_{02} = -2/5$ and $t_{30} = t_{03} = 1/15$, and so on, generalizing to the case

$$H_{\text{eff}}^{(2n)} = K_x^{2n} + K_y^{2n} \quad (8)$$

We find the perturbative, finite-size eigenstates of these effective hamiltonians numerically, and display the trace inequality of their ground states in Fig. (4). We find that the trace inequality is maximum for $2n = 6$, and that for larger values of n it decreases monotonically at least until $2n = 30$.

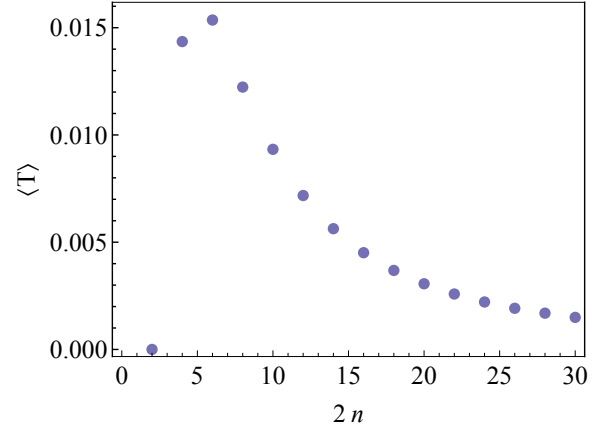


FIG. 4. Trace inequality $\langle T \rangle = 2 \langle a^\dagger a \rangle$ for the ground state band of the hamiltonian $H^{(2n)}$. When $n = 1$, this is the Landau level hamiltonian for which the lowest-lying band has $\langle T \rangle = 0$ as shown.

A. Non-perturbative corrections and uniformity of band geometry

In the perturbative treatment we have employed so far, we expand about a band minimum to obtain an effective mean-field hamiltonian. While this method gives corrections to the energy levels due to change in shape of the effective dispersion near the minimum, it neglects corrections arising from the discreteness of the lattice. In particular, since Landau levels have perfectly uniform energy dispersion, Berry curvature, and Fubini-Study metric, any fluctuations in these must come from non-perturbative corrections. These non-perturbative corrections arise from tunnelling between band minima, so intuitively we may expect them to decay exponentially in width of the potential barrier.

Our current situation is not much different, because the WKB – specifically, physical optics – approximation can be employed for any order differential or difference equation. That is, we may use the WKB ansatz

$$\psi(x) = \exp \left[\frac{1}{\phi} (S_0(x) + \phi S_1(x)) \right], \quad (9)$$

for any order Harper-type equation with the same constraints on the region of validity that apply to the physical optics approximation for the usual Harper equation.³⁸ As a tractable

example of how the WKB solution changes when we incorporate longer-range hopping terms in the Harper equation, we consider the difference equation

$$\psi(x + n\phi) + \psi(x - n\phi) = \cosh q(x) \psi(x)$$

where we have defined $\cosh q(x) = -\epsilon - V(x)$. This equation would arise if we included only hopping by n lattice sites in the x direction. Substituting the WKB ansatz and comparing orders in ϕ yields solutions

$$\psi_{\text{exp}}^{\pm} = \frac{1}{\sqrt{\sinh(q(x))}} \exp\left(\pm \frac{1}{n\phi} \int^x ds q(s)\right).$$

in the classically-forbidden region. In this simple case, the only effect of the longer-range hoppings is to modify the argument of the exponential by a factor $O(1)$ in ϕ . We expect but do not prove that this is the generic behavior of such solutions. For each of the cases we consider in this article, we observe overall exponential decay of the amplitudes of fluctuations on the MBZ in numerics. We plot examples of this exponential decay in Fig. 5. For this reason, we neglect non-

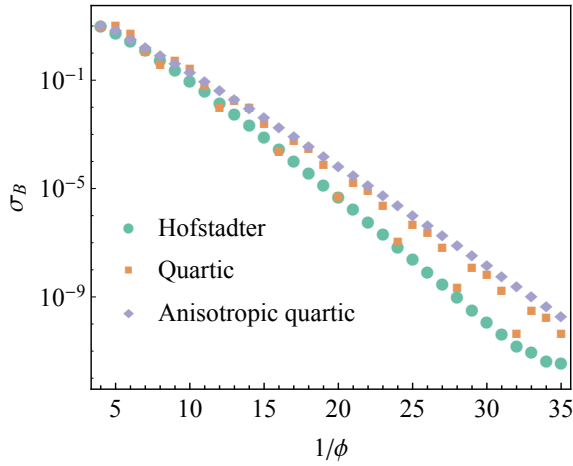


FIG. 5. RMS fluctuation σ_B of Berry curvature B from its average value on the MBZ.

perturbative fluctuations. Since we measure deviations of our Chern bands from Landau levels by band geometric quantities, and since we treat the Berry curvature and Fubini-Study metric as uniform on the MBZ, deviations from Landau level behavior are measured predominantly by the inequalities ()

B. Hamiltonians with no h_0 term

That the overlap of the groundstate of the zero-quadratic model with the LLL is large is not surprising, given the large weight of the Landau hamiltonian h_0 in (5). We might ask whether it is possible to eliminate this term entirely, and what impact this has on the spectrum. In fact, we can isolate the $a^4 + a^{\dagger 4}$ term by choosing $t_{01} = t_{10} = 1$, $t_{02} = t_{20} = \frac{1}{8}$, and $t_{11} = -\frac{3}{4}$, giving

$$H_{\text{eff}} = \frac{3}{2} + \frac{\phi^2}{4} (a^4 + a^{\dagger 4}).$$

This case is distinct from the cases we have considered so far because we are expanding about a local maximum instead of a minimum in the dispersion. The spectrum of this hamiltonian is not bounded from below, so we cannot find its ground states. However, there is a set of degenerate zero-energy states. While we were unable to obtain an analytical form for the coefficients in the LL basis for the ground state of (5), the fact that the states here have exactly zero energy makes the current problem tractable. We find that there are four zero-energy states obtained by unitary transformations of $|0\rangle$, $|1\rangle$, $|2\rangle$, and $|3\rangle$, and present an analytical calculation of one of the zero-energy states in Appendix B. Although this hamiltonian does not depend on h_0 , the state $|\tilde{0}\rangle = U|0\rangle$ maintains a large overlap $\langle \tilde{0} | 0 \rangle \approx 0.987926$ with the Landau level ground state.

C. Anisotropic models

In the foregoing, we considered only models invariant under C_4 symmetry. Of course, generic models will not maintain this symmetry, so we should consider the effects of anisotropy. Rather than treating fully generic models, we consider two straightforward generalizations of the above models that capture essential features. First, we have models in which K_x and K_y both enter the effective hamiltonian at the same order to lowest order in ϕ , but with different coefficients. The simplest example of such a model is the Hofstadter model with different coefficients in the x and y directions, with

$$H_{\text{eff}} = \frac{\alpha}{2} K_x^2 + \frac{1}{2\alpha} K_y^2.$$

This anisotropic Landau level hamiltonian and its bands have been studied in relation to nematic quantum Hall phases.

Separately, we also consider the case in which we eliminate terms in the effective hamiltonian at different orders in ϕ . That is, we choose the hoppings so that

$$H_{\text{eff}} = h_1 K_x^{2m} + h_2 K_y^{2n}.$$

For example, with $t_{20} = 0$ and $t_{02} = -t_{01}/4$,

$$H_{\text{eff}} = t_{10} \left(-4 + K_x^2 - \frac{1}{12} K_x^4 \right) + t_{01} \left(-3 + \frac{1}{4} K_y^4 \right),$$

or, with $t_{01} = t_{10} = 1$,

$$H_{\text{eff}} = -7 + K_x^2 - \frac{1}{12} K_x^4 + \frac{1}{4} K_y^4$$

For small ϕ , the effective hamiltonian will be dominated by the quadratic term, and we might expect that the problem becomes effectively one-dimensional as $\phi \rightarrow 0$. Calculating the Chern number c_1 for the lowest band of the lattice model, we find that $|c_1| = 1$ even for ϕ as small as $1/1350$.

IV. INTERACTIONS AND STABILITY OF FQH STATES

By consideration of the algebra of density operators projected to Chern bands – the analogue of the well-known Girvin-MacDonald-Platzmann (GMP) algebra of the FQHE¹⁵ – one can infer quantitative measures of deviations from “ideal” LL behavior.^{16,17} Specifically, if the Berry curvature and Fubini-Study metric are uniform over the MBZ, then the algebra of projected density operators closes to $O(k^3)$. If, in addition to the uniformity of B and g , $D(\mathbf{k}) = 0$ (or equivalently $T(\mathbf{k}) = 0$), this algebra closes to all orders in k . This suggests a connection between these geometric observables and the stability of the many-body gapped liquid phase in lattice QH systems, which is supported by numerical evidence in both Chern insulator¹⁸ and Harper-Hofstadter²⁰ regimes. In FCI models however, fluctuations in band-geometric densities are generically non-negligible, and are correlated with saturation of the inequalities. By contrast, in the weak-field limit of the Hofstadter model, we may neglect fluctuations, but the lack of tunable model parameters means that we cannot vary the band-geometric inequalities independently from ϕ .

The more generic tight-binding models we study in this work therefore provide a new regime in which to study the effects of band geometry on the stability of lattice FQH phases. Considering, for example, the model (4), we can set ϕ to be arbitrarily small and neglect fluctuations while varying t_2 and hence $\langle T \rangle$.

To study the fractional quantum Hall effect, we introduce a repulsive, two-body interaction potential on the lattice,

$$V = \sum_{\mathbf{m}, \mathbf{n}} v_{\mathbf{mn}} c_{\mathbf{m}}^\dagger c_{\mathbf{m}} c_{\mathbf{n}}^\dagger c_{\mathbf{n}}.$$

We fractionally fill a single band of energy eigenstates with N_p particles. Each band contains $N_s = A_{\text{tot}}/A_{\text{MUC}}$ states, and the filling fraction $\nu = N_p/N_s$. We work within a single band with projector P ; that is, we diagonalize the interaction hamiltonian $H_{\text{int}} = PVP$.

We study many-body phases of bosons at filling fraction $\nu = 1/2$ and fermions at $\nu = 1/3$.

V. SPATIALLY-INHOMOGENEOUS EM RESPONSE

The perturbative response of QH fluids to static, spatially homogeneous electric fields is a key phenomenological feature of such fluids. This response is measured by the conductivity tensor σ relating the electric current density \mathbf{J} and perturbative electric field \mathbf{E} ,

$$J_a = \sigma_{ab} E_b. \quad (10)$$

In particular, one is interested in the transverse, or Hall, conductivity σ_{xy} , which takes the universal value

$$\sigma_{xy} = \sigma_H = \frac{\nu e^2}{2\pi\hbar}$$

in quantum Hall fluids at filling fractional ν .

Another universal phenomenological feature of QH fluids is the Hall viscosity η_H .^{7,8,39} Recent work has shown that the perturbative response to spatially *inhomogeneous* electric fields is related to the Hall viscosity.^{40,41} The universal contribution to the Hall viscosity in a QH fluid on a surface with zero scalar curvature is³⁹

$$\eta_H = \frac{1}{2} \hbar \bar{s} \rho_0,$$

where ρ_0 is the mean density and \bar{s} is the mean orbital angular momentum or topological spin of the fluid. For example, a Laughlin fluid with $\nu = \frac{1}{2k+1}$ has,

$$\bar{s} = k + \frac{1}{2}.$$

If we consider the finite-wavevector version of (10) above

$$J_a(\mathbf{q}) = \sigma_{ab}(\mathbf{q}) E_b(\mathbf{q}),$$

then the transverse conductivity is

$$\frac{\sigma_{xy}(\mathbf{q})}{\sigma_H} = 1 + (q\ell)^2 \left(\frac{\eta_H}{\hbar\rho_0} - \frac{B^2}{2\nu u_0} \frac{\partial^2 u}{\partial B^2} \right).$$

Where $u(B)$ is the energy density as a function of magnetic field, and u_0 is the LLL energy density

$$u_0 = \frac{\hbar\omega/2}{2\pi\ell^2}.$$

Ref. 42 presents a derivation of two transverse current responses in Chern bands to an applied inhomogeneous electric field. The first is the current per state or current per orbital, which is the current response of a single filled state within a Chern band,

$$\begin{aligned} \langle I_{yn} \rangle = & -i \sum_{m \neq n} \langle n, k | [y, H] | m, k \rangle \frac{\langle m, k | V(x) | n, k \rangle}{E_n - E_m} \\ & + \text{h.c.}, \end{aligned} \quad (11)$$

with current operator $I_y = -i[y, H]$. The second response is the real-space current density,

$$\begin{aligned} J_{yn}(\mathbf{r}_0) = & \sum_{k, m \neq n} \langle n, k | j_y(\mathbf{r}_0) | m, k \rangle \frac{\langle m, k | V(x) | n, k \rangle}{E_n - E_m} \\ & + \text{h.c.}, \end{aligned} \quad (12)$$

where $j_y(\mathbf{r}_0)$ is the symmetrized current density operator

$$j_y(\mathbf{r}_0) = \frac{1}{2} (I_y \delta(\mathbf{r} - \mathbf{r}_0) + \delta(\mathbf{r} - \mathbf{r}_0) I_y).$$

From the current density response, we can calculate the transverse conductivity $\sigma_{xy}(\mathbf{q})$. This expression for $J_{yn}(\mathbf{r}_0)$ is equivalent to that obtained by a linear response calculation. The factor of H in the current per orbital cancels the energy denominator, so that $\langle I_y n \rangle$ depends only on the band projectors and not on the energy dispersion. In contrast, this cancellation does not occur in the case of the current density. For a generic

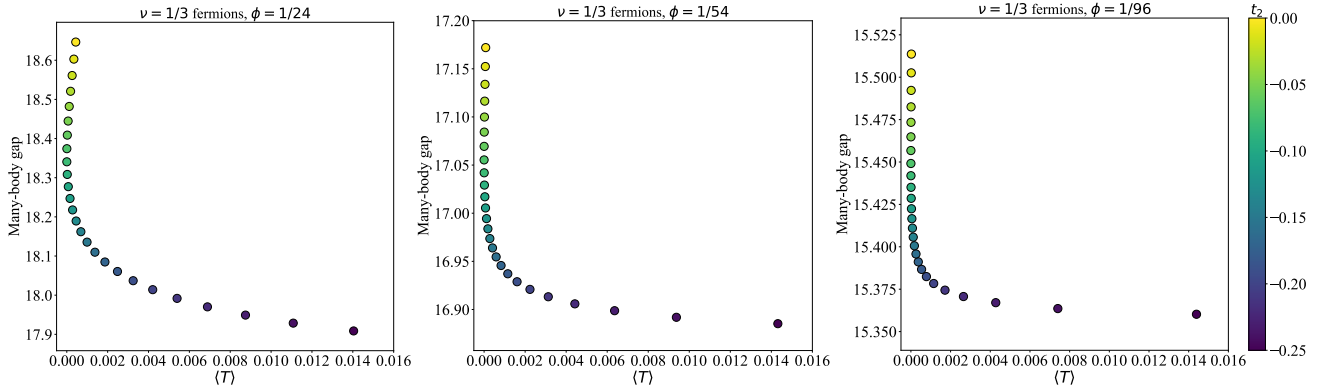


FIG. 6.

scalar potential $V(x)$, we can write a Taylor series expansion about x_0 ,

$$V(x) = \sum c_p (x - x_0)^p.$$

Then the current per orbital in the n -th Landau level in response to the potential $V(x)$ is, in terms of the expansion coefficients c_p ,

$$\begin{aligned} \langle I_{yn} \rangle = & -c_1 \ell^2 - 3c_3 \ell^4 \left(n + \frac{1}{2} \right) \\ & - \frac{15}{2} c_5 \ell^6 \left(n^2 + n + \frac{1}{2} \right) + \dots, \end{aligned} \quad (13)$$

and the current density is

$$\begin{aligned} J_{yn}(\mathbf{r}_0) = & -\frac{1}{2\pi\ell^2} [c_1 \ell^2 + 9c_3 \ell^4 \left(n + \frac{1}{2} \right) \\ & + \frac{5}{2} c_5 \ell^6 (11 + 30n + 30n^2) + \dots] \end{aligned} \quad (14)$$

In the case of non-Landau level models, the above expressions (11) and (12) still hold, with the caveats that we must calculate the current operator $-i[y, H]$ using the non-Landau

hamiltonian and interpret the states $|n, k\rangle$ as eigenstates of this hamiltonian. We have seen that we can obtain these perturbative eigenstates numerically by considering a finite-dimensional truncation of the hamiltonian written in the Landau level basis. In this way, we can numerically calculate these current responses for the case of our non-Landau bands. This calculation is carried out in detail for C_4 symmetric models in Ref. 42.

Here, we compute the corrections to the Landau level responses (13) and (14) for the hamiltonians

$$H^{(2n)} = K_x^{2n} + K_y^{2n}.$$

Writing $|\lambda^{(2n)}\rangle$ for the eigenstates of this hamiltonian, we obtain the current per orbital

$$\begin{aligned} \langle I_{y\lambda} \rangle^{(2n)} = & 2 \sum_{\substack{\mu \neq \lambda \\ p}} (-1)^p c_p \ell^{2p} \langle \lambda^{(2n)} | K_y^{2n-1} | \mu^{(2n)} \rangle \times \\ & \frac{\langle \mu^{(2n)} | K_y^p | \lambda^{(2n)} \rangle}{E_\lambda - E_\mu} + \text{h.c.} \end{aligned}$$

and current density

$$\langle J_{y\lambda} \rangle^{(2n)} = \frac{1}{\pi\ell^2} \sum_{\substack{\mu \neq \lambda \\ p, r}} (-1)^r c_p^2 \ell^{2p} \binom{p}{p-r} \langle \lambda^{(2n)} | K_y^{2n-1+p-r} | \mu^{(2n)} \rangle \frac{\langle \mu^{(2n)} | K_y^r | \lambda^{(2n)} \rangle}{E_\lambda - E_\mu} + \text{h.c.}$$

The effect of these corrections amounts to employing the expressions (13) and (14) with changes to the numerical factors multiplying each expansion coefficient c_p . For example, in the Landau level case, the numerical factors multiplying c_1 , c_3 , and c_5 in Eq. (13) are respectively 1, $3/2$, and $15/4$ for $n = 0$, and 1 , $9/2$, $75/4$ for $n = 1$. The factor multiplying the coefficient c_1 , which corresponds to the spatially-homogeneous component of the electric field, does not change

from its Landau level value. In Fig. (7), we plot the numerical factors multiplying c_3 and c_5 in the current per orbital for some eigenstates $|\lambda\rangle$ of $H^{(2n)}$; we plot the same for the current density in Fig. (8).

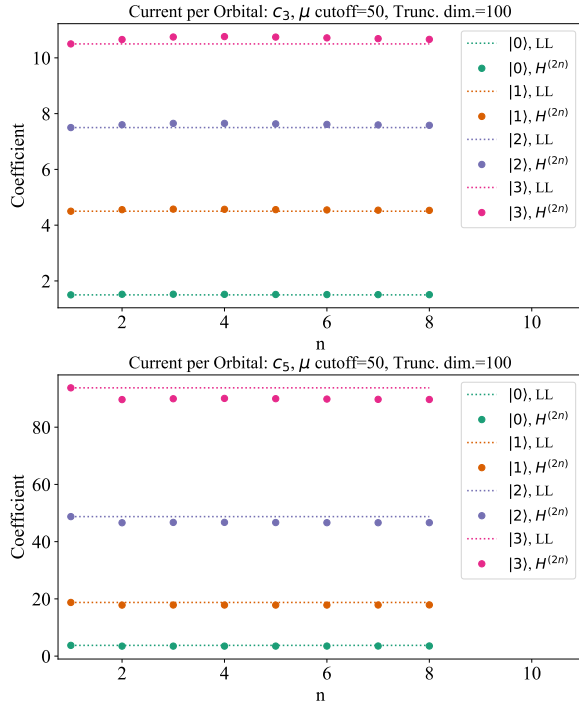


FIG. 7.

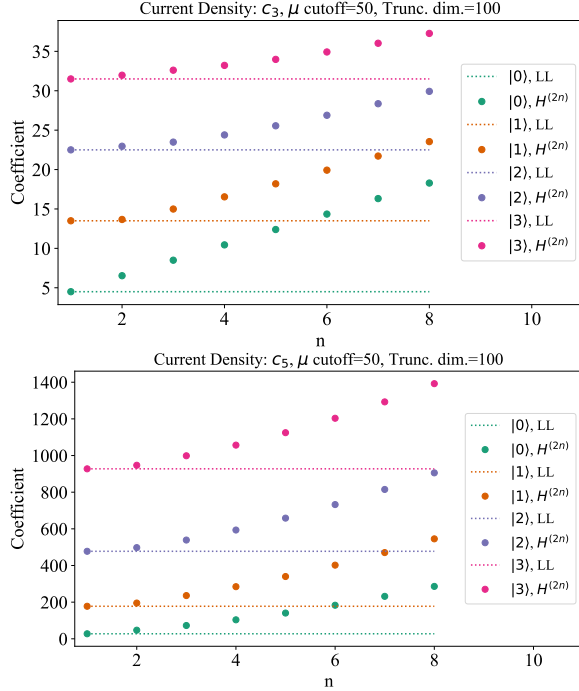


FIG. 8.

VI. CONCLUSION

In conclusion, we have constructed a Harper-Hofstadter model with cyclotron orbits that are distinct from Landau levels in the continuum limit. This provides a regime in which to study the quantum Hall effect that is distinct from both the Landau level 2DEG and FCI models.

While we have focused on a particular choice of hopping amplitudes, by including longer-range hoppings and tuning them appropriately, one may obtain arbitrary inversion-symmetric dispersion relations.

One drawback of our numerical approach is that we diagonalize the many-body interaction hamiltonian on a lattice. While this is not a problem in the FCI regime, it may obscure the physics in the continuum regime, for example by gapping potential symmetry-breaking Goldstone modes that would be gapless in the continuum. Using DMRG or other numerical techniques that do not rely directly on a tight-binding description may remedy this. Another drawback of constructing continuum bands from lattice model is that the continuum models inherit non-generic point-group symmetries from the lattice geometry, so that we do not obtain fully generic bands in this way.

ACKNOWLEDGMENTS

The authors thank Tom Jackson for collaboration on related work and for his band geometry code. We also thank authors of the DiagHam package, which was used in this work.

* dbauer@physics.ucla.edu

¹ D. Yoshioka, *The Quantum Hall Effect*, 1st ed. (Springer, 2002).

² E. Fradkin, *Field Theories of Condensed Matter Physics*, 2nd ed. (Cambridge University Press, 2013).

³ R. B. Laughlin, *Phys. Rev. Lett.* **50**, 1395 (1983).

⁴ D. J. Thouless, M. Kohmoto, M. P. Nightingale, and M. den Nijs, *Phys. Rev. Lett.* **49**, 405 (1982).

⁵ F. D. M. Haldane, *Phys. Rev. Lett.* **107** (2011).

- ⁶ S. Johri, Z. Papić, P. Schmitteckert, R. N. Bhatt, and F. D. M. Haldane, *New J. Physics* **18**, 025011 (2016).
- ⁷ J. E. Avron, R. Seiler, and P. G. Zograf, *Phys. Rev. Lett.* **75**, 697 (1995).
- ⁸ I. V. Tokatly and G. Vignale, *Phys. Rev. B* **76** (2007).
- ⁹ N. Read, *Phys. Rev. B* **79** (2009).
- ¹⁰ F. D. M. Haldane, *arXiv:0906.1854* (2009).
- ¹¹ E. J. Bergholtz and Z. Liu, *Int. J. Mod. Phys. B* **27**, 1330017 (2013).
- ¹² S. A. Parameswaran, R. Roy, and S. L. Sondhi, *Comptes Rendus Physique* **14**, 816 (2013).
- ¹³ H. Shapourian, T. L. Hughes, and S. Ryu, *Phys. Rev. B* **92** (2015).
- ¹⁴ J. Zak, *Physical Review* **134**, A1607 (1964).
- ¹⁵ S. M. Girvin, A. H. MacDonald, and P. M. Platzman, *Phys. Rev. B* **33**, 2481 (1986).
- ¹⁶ S. A. Parameswaran, R. Roy, and S. L. Sondhi, *Phys. Rev. B* **85** (2012).
- ¹⁷ R. Roy, *Phys. Rev. B* **90** (2014).
- ¹⁸ T. S. Jackson, G. Möller, and R. Roy, *Nature Communications* **6**, 8629 (2015).
- ¹⁹ M. Claassen, C. H. Lee, R. Thomale, X.-L. Qi, and T. P. Devereaux, *Phys. Rev. Lett.* **114**, 236802 (2015).
- ²⁰ D. Bauer, T. S. Jackson, and R. Roy, *Phys. Rev. B* **93** (2016).
- ²¹ C. H. Lee, M. Claassen, and R. Thomale, *Phys. Rev. B* **96**, 165150 (2017).
- ²² F. D. M. Haldane and Y. Shen, *arXiv:1512.04502* (2015).
- ²³ E. M. Spanton, A. A. Zibrov, H. Zhou, T. Taniguchi, K. Watanabe, M. P. Zaletel, and A. F. Young, *Science* (2018).
- ²⁴ G. Jotzu, M. Messer, R. Desbuquois, M. Lebrat, T. Uehlinger, D. Greif, and T. Esslinger, *Nature* **515**, 237 EP (2014).
- ²⁵ M. Aidelsburger, M. Lohse, C. Schweizer, M. Atala, J. T. Barreiro, S. Nascimbène, N. R. Cooper, I. Bloch, and N. Goldman, *Nat. Phys.* **11**, 162 (2014).
- ²⁶ M. Aidelsburger, M. Atala, M. Lohse, J. T. Barreiro, B. Paredes, and I. Bloch, *Phys. Rev. Lett.* **111**, 185301 (2013).
- ²⁷ N. Fläschner, B. S. Rem, M. Tarnowski, D. Vogel, D.-S. Lühmann, K. Sengstock, and C. Weitenberg, *Science* **352**, 1091 (2016).
- ²⁸ A. Kol and N. Read, *Phys. Rev. B* **48**, 8890 (1993).
- ²⁹ R. N. Palmer and D. Jaksch, *Phys. Rev. Lett.* **96** (2006).
- ³⁰ P. G. Harper, *Proc. Phys. Soc. A* **68**, 879 (1955).
- ³¹ M. Y. Azbel, *Soviet Physics JETP* **19**, 634 (1964).
- ³² D. Hofstadter, *Phys. Rev. B* **14**, 2239 (1976).
- ³³ F. D. M. Haldane, *Phys. Rev. Lett.* **61**, 2015 (1988).
- ³⁴ J. McGreevy, B. Swingle, and K.-A. Tran, *Phys. Rev. B* **85** (2012).
- ³⁵ F. Harper, S. H. Simon, and R. Roy, *Phys. Rev. B* **90**, 075104 (2014).
- ³⁶ G. Palumbo, *Eur. J. Phys.* **133**, 23 (2018).
- ³⁷ A. Eckardt, *Rev. Mod. Phys.* **89**, 011004 (2017).
- ³⁸ C. M. Bender and S. A. Orszag, *Advanced Mathematical Methods for Scientists and Engineers I: Asymptotic Methods and Perturbation Theory* (Springer-Verlag, New York, 1999).
- ³⁹ N. Read, *Phys. Rev. B* **79**, 045308 (2009).
- ⁴⁰ C. Hoyos and D. T. Son, *Physical Review Letters* **108** (2012).
- ⁴¹ B. Bradlyn, M. Goldstein, and N. Read, *Physical Review B* **86** (2012).
- ⁴² F. Harper, D. Bauer, T. S. Jackson, and R. Roy, *arXiv:1807.00970* (2018).

Appendix A: Weak-field effective hamiltonian for Hofstadter model C_4 symmetric NNN hopping

For completeness, we reproduce here the Hofstadter model with all next-nearest-neighbor (NNN) hopping terms that respect C_4 symmetry, including the hopping diagonally across a plaquette. The tight-binding hamiltonian is

$$H_0 = -t_1 (T_x + T_y) - t_2 (T_x^2 + T_y^2) - t_3 (T_x T_y + T_y T_x) + \text{h.c.}$$

We can write this in terms of the generators K_a as

$$H_0 = -2t_1 [\cos(K_x) + \cos(K_y)] - 2t_2 [\cos(2K_x) + \cos(2K_y)] - 4t_3 \cosh\left(\frac{\phi}{2}\right) \cos(K_x + K_y).$$

The factor of $\cosh(\phi/2)$ is non-universal and results from our ordering prescription. Expanding to quartic order, we obtain the small- ϕ effective hamiltonian

$$H_{\text{eff}} = h_{ab} K_a K_b + \lambda_{abcd} K_a K_b K_c K_d$$

with coefficients

$$h_{11} = h_{22} = t_1 + 4t_2 + 2t_3, \\ h_{12} = 2t_3,$$

and

$$\lambda_{1111} = \lambda_{2222} = -\frac{1}{3} \left(\frac{t_1}{4} + 4t_2 + \frac{t_3}{2} \right), \\ \lambda_{1112} = \lambda_{1222} = -t_3/3, \\ \lambda_{1122} = -t_3/2.$$

Appendix B: Zero-energy states for $a^4 + a^{\dagger 4}$ hamiltonian

We try to obtain an analytic expression for the lowest energy wavefunction of a particular quartic model. We take the Hamiltonian

$$\hat{H} = \omega [a^4 + (a^\dagger)^4]$$

and write a general wavefunction as

$$|\psi\rangle = \sum_k C_k |k\rangle$$

as a sum over Landau level states. The eigenvalue equation becomes

$$\hat{H} |\psi\rangle = \omega \sum_k C_k [\sqrt{k(k-1)(k-2)(k-3)} |k-4\rangle + \sqrt{(k+1)(k+2)(k+3)(k+4)} |k+4\rangle] \\ = E \sum_k C_k |k\rangle.$$

Taking inner products with different Landau level states yields

$$\omega [C_{4(p+1)} \alpha_{-4}(4(p+1)) + C_{4(p-1)} \alpha_{+4}(4(p-1))] = E C_{4p},$$

where we have defined

$$\alpha_{-}(k) = \sqrt{k(k-1)(k-2)(k-3)} \\ \alpha_{+}(k) = \sqrt{(k+1)(k+2)(k+3)(k+4)}.$$

We first try to obtain a state with energy $E = 0$. Substituting this into some of the coefficient equations, we find

$$C_4 = 0 \\ C_8 = -C_0 \frac{\alpha_{+4}(0)}{\alpha_{-4}(8)} \\ C_{12} = 0 \\ C_{16} = -C_8 \frac{\alpha_{+4}(8)}{\alpha_{-4}(16)} \\ = C_0 \frac{\alpha_{+4}(8)\alpha_{+4}(0)}{\alpha_{-4}(16)\alpha_{-4}(8)}.$$

The pattern of coefficients continues in the same manner. We define

$$\beta(k) = \frac{\alpha_{+4}(8(k-1))}{\alpha_{-4}(8k)}$$

so that

$$C_8 = -\beta(1)C_0 \\ C_{16} = +\beta(2)\beta(1)C_0 \\ \vdots \\ C_{8p} = (-1)^p C_0 \prod_{k=1}^p \beta(k) \\ \equiv \gamma(p)C_0,$$

where we have defined $\gamma(p)$ in the final line. Mathematica simplifies the function γ to

$$\gamma(n) = \frac{\sqrt[4]{\frac{2}{\pi}} \Gamma\left(\frac{7}{8}\right) \sqrt{\Gamma\left(n + \frac{9}{8}\right) \Gamma\left(n + \frac{5}{4}\right) \Gamma\left(n + \frac{11}{8}\right) \Gamma\left(n + \frac{3}{2}\right)}}{\Gamma\left(\frac{1}{8}\right) \sqrt{\Gamma\left(n + \frac{13}{8}\right) \Gamma\left(n + \frac{7}{4}\right) \Gamma\left(n + \frac{15}{8}\right) \Gamma(n+2)}},$$

with

$$\Gamma(z) = \int_0^\infty x^{z-1} e^{-x} dx.$$

We now have both a recursive and a non-recursive relation for the coefficient C_{8p} (with all other $C_k = 0$). The complete wavefunction is

$$|\psi\rangle = \sum_k C_k |k\rangle \\ = C_0 \sum_k \gamma(k) |k\rangle,$$

which leads to the normalisation condition

$$1 = |C_0|^2 [1 + |\gamma(1)|^2 + |\gamma(2)|^2 + \dots].$$

Using Mathematica, we find

$$\frac{1}{|C_0|^2} = {}_4F_3 \left(\left[\frac{1}{8}, \frac{1}{4}, \frac{3}{8}, \frac{1}{2} \right], \left[\frac{5}{8}, \frac{3}{4}, \frac{7}{8} \right], 1 \right),$$

where ${}_4F_3(a; b; z)$ is a generalised hypergeometric function. Solving for C_0 , we find

$$C_0 = 0.987926,$$

which agrees very well with numerics.

